CHEMBIOCHEM

DOI: 10.1002/cbic.200900003

New Approach for Local Structure Analysis of the Tyrosine Domain in Proteins by Using a Site-Specific and Polarity-Sensitive Fluorescent Probe

Suming Chen, Xiaohua Li, and Huimin Ma*[a]

The design and synthesis of a novel long-wavelength polarity-sensitive fluorescence probe, 6-[9-(diethylamino)-5-oxo-5*H*-benzo[α]phenoxazin-2-yloxy]hex-2-enyl acetate, for the selective modification of tyrosine residues with the goal of providing local information on tyrosine domains in proteins, is reported. This probe comprises a polarity-sensitive Nile red fluorophore and an active π-allyl group that can form π-allylpalladium complexes and react selectively with tyrosine residues. The probe has the following features: 1) it has a long-wavelength emission of >550 nm, thanks to which interference from short-wavelength fluorescence from common biological matrixes can be avoided; 2) the maximum emission wavelength is sensitive only to polarity and not to pH or temperature; this allows the accurate determination of local polarity; and 3) it is a neutral, uncharged molecule, and does not disturb the overall charge of the labelled protein. With this probe the polarity and conformation changes of the Tyr108 domain in native and in acid- and heat-denatured bovine Cu/Zn superoxide dismutase were detected for the first time. It was found that the polarity of the Tyr108 domain hardly alters on acid denaturation between pH 4 and 9. However, heat denaturation caused the Tyr108 domain to be more hydrophobic, and was accompanied by an irreversible aggregation of the protein. In addition, the probe-binding experiments revealed that the surface of the protein becomes more hydrophobic after thermal denaturation; this can be ascribed to the formation of the more hydrophobic aggregates. This strategy might provide a general approach for studying the local environment changes of tyrosine domains in proteins under acid or heat denaturation conditions.

Introduction

The function of a protein depends mainly on its structure.[1,2] The occurrence even of only partial structural disorder/misfolding can lead to diseases such as Alzheimer's, Parkinson's and prion diseases.[3] Analysis of the local structure of a protein (e.g., obtaining information on local environmental changes during folding/unfolding) can thus be crucial for better understanding of the protein's properties.

On the other hand, much attention has been paid to tyrosine domains, not only because tyrosine is one of the primary amino acids in proteins, but also because modification of tyrosine residues in these domains plays a special role in many important biochemical processes—tyrosine phosphorylation, for example, is considered to be one of the key steps in signal transduction and regulation of enzymatic activity.[4–8] In addition, conformational change of tyrosine in an active site is usually related to alteration of an enzyme's activity and kinetics.[9–11] Therefore, the study of tyrosine domains could provide insights into the function of proteins in complex biological processes.

Fluorescent probes have been widely used for biological studies.[12–16] In particular, environment-sensitive fluorescent probes combined with site-specific labelling techniques play an important role in structural analyses of proteins because of their great temporal and spatial sampling capability.[17–26] This technology can also be applied to the study of conformation changes in tyrosine domains and could be useful for comprehensive understanding of the functions of these domains. Clearly, the prerequisites for conducting such studies are to develop corresponding tyrosine-specific labelling methods and excellent spectroscopic probes.

Modification of tyrosine residues in proteins is usually achieved either through acylation or electrophilic aromatic substitution pathways.[27] However, these approaches suffer from disadvantages, including low selectivity and radioactive risks.[28–32] Recently, transition-metal-mediated reactions have emerged as a promising set of strategies for protein modification.[33–36] Tilley and Francis reported a novel tyrosine labelling method using π-allylpalladium complexes.[34] In one such approach, efficient tyrosine labelling under mild conditions through palladium carboxylate catalysis was observed, and most importantly, the reactions of π-allylpalladium complexes are highly selective for tyrosine out of the various amino acid residues encountered in proteins.[34] Nevertheless, the rhodamine-type fluorescent compound used in that study is insensitive to changes in environmental factors and thus cannot provide detailed information on the tyrosine domain.

[a] *S. Chen, Dr. X. Li, Prof. Dr. H. Ma*
Beijing National Laboratory for Molecular Sciences
Institute of Chemistry, Chinese Academy of Sciences
Beijing 100190 (China)
Fax: (+86) 10-62559373
E-mail: mahm@iccas.ac.cn

Supporting information for this article is available on the WWW under http://dx.doi.org/10.1002/cbic.200900003.

Excellent environment-sensitive fluorescent probes that are suitable for local conformation studies should possess the following properties: 1) the fluorescence response should be sensitive only to one environmental factor (polarity, pH or temperature) and not to multiple factors, so that cross-interference can be eliminated; 2) it should have a long-wavelength fluorescence, to avoid the influence of short-wavelength fluorescence from proteins; and 3) it should be a neutral, uncharged molecule, so as not to disturb the overall charge of a native protein.

To meet these requirements for tyrosine domain analysis, we have taken advantage of π-allylpalladium complexes to design a novel long-wavelength, polarity-sensitive fluorescence probe, 6-[9-(diethylamino)-5-oxo-5*H*-benzo[α]phenoxazin-2-yloxy]hex-2-enyl acetate (DBHA, Scheme 1). The probe comprises a Nile red fluorophore and an active π-allyl group, the properties of which have been characterized and indicate that the probe is suitable for local structural studies. Here, this application is demonstrated in the detection of local polarity and conformational changes in the unique tyrosine (Tyr108) domain in the bovine erythrocyte Cu/Zn superoxide dismutase (SOD).

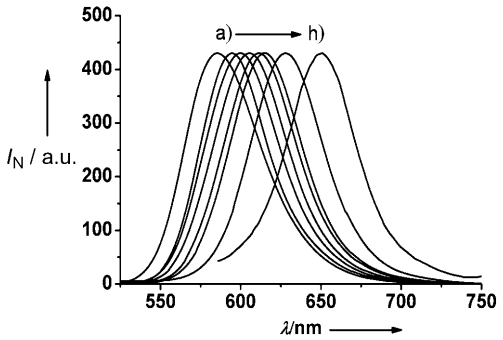

Figure 1. Normalized fluorescence emission spectra of DBHA in various solvents. The curves represent: a) ethyl acetate, b) dichloromethane, c) acetone, d) acetonitrile, e) methanol, f) DMF, g) DMSO, and h) water; in this medium, the higher background fluorescence at about 585 nm was due to scattering. I_N denotes the normalized fluorescence intensity.

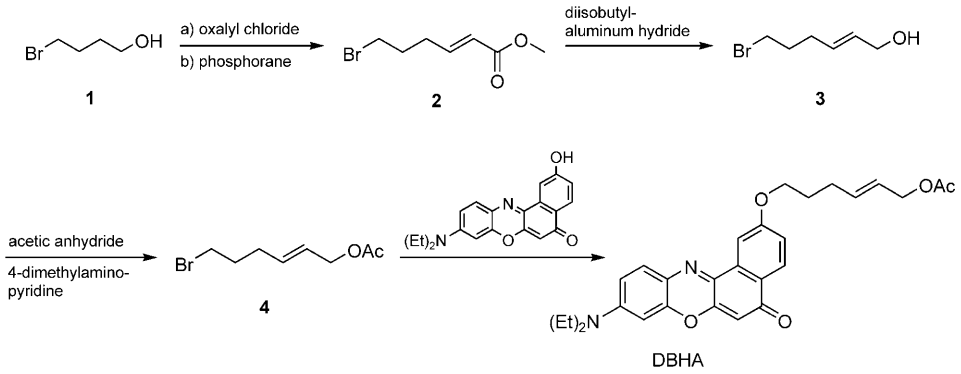

Scheme 1. Synthesis of 6-[9-(diethylamino)-5-oxo-5*H*-benzo[α]phenoxazin-2-yloxy]hex-2-enyl acetate (DBHA).

Results and Discussion

Solvent effects on the fluorescent properties of DBHA

The fluorescent properties of DBHA were examined in different solvents. As shown in Figure 1, the emission maxima of DBHA are generally located in the red region of the spectrum and vary from 584 to 650 nm, which should allow interference from short-wavelength fluorescence from common biological matrixes to be efficiently avoided. This property is essential for biomacromolecular studies.

Detailed information about the effect of solvents is given in Table 1. As can be seen, the fluorescence emission maximum of DBHA shifts to a longer-wavelength region with the increasing dielectric constant of the solvents, except in the case of alcohols, which might specifically interact with Nile red through hydrogen bonding.[35,36] In contrast, the fluorescence quantum yield decreases with increasing solvent polarity. In the nonpolar medium chloroform, for example, DBHA exhibits a strong emission at 584 nm with a quantum yield of 0.27, whereas in water the maximum emission shifts bathochromically to 650 nm, and is accompanied by a decrease in the quantum yield to 0.0018. This kind of solvatochromic effect is typical, and is consistent with the phenomenon observed for its parent compound Nile red.[35–38] The relationship between the shift of maximum emission wavelength ($\Delta\lambda_{em}$) and the dielectric constants (D) of the solvents (not including methanol and ethanol) displays a good linearity ($\Delta\lambda_{em} = 69.4–0.84\times D$; $n = 9$, $\gamma = 0.986$); this suggests that the alteration of local polarity in a protein should be quantitatively determinable through monitoring the shift of the maximum emission wavelength of a DBHA-labelled protein.

Table 1. Spectroscopic properties of DBHA in various solvents.

Solvent	D[a]	λ_{ex} [nm]	λ_{em} [nm]	$\Delta\lambda_{em}$[b] [nm]	Φ[c]
chloroform	4.81	520	584	66	0.27
ethyl acetate	6.08	517	585	65	0.35
tetrahydrofuran	7.52	521	587	63	0.26
dichloromethane	9.14	531	595	55	0.29
acetone	21.0	525	600	50	0.27
ethanol	25.3	542	623	27	0.13
methanol	33.0	547	628	22	0.10
acetonitrile	36.6	529	605	45	0.14
DMF	38.2	537	611	39	0.19
DMSO	47.2	545	620	30	0.14
water (sodium phosphate buffer)	80.1	585	650	0	0.0018

[a] The dielectric constants (D) of the solvents were obtained from the literature.[39] [b] Shift of maximum emission wavelength: $\Delta\lambda_{em} = \lambda_{em}$ (in water) $-\lambda_{em}$ (in an organic solvent). [c] Fluorescence quantum yield (Φ) was determined with rhodamine B as a standard ($\Phi = 0.71$ in ethanol).[40,41]

Effects of acidity and temperature on the fluorescence of DBHA

The effects of acidity and temperature on the fluorescence properties of DBHA were examined, because these two factors are often used to denature proteins. Figure 2 shows the fluorescence spectra of DBHA in different pH media from pH 2 to 9. As can be seen, the fluorescence intensity of DBHA increases with the rise in pH from 2 to 5, and then reaches a near-plateau; however, its maximum emission wavelength (λ_{em}) hardly shifts (fluctuation $\leq$4 nm). Similarly, a change in temperature from 20 to 80 °C affects the fluorescence intensity of DBHA in a more complicated manner (Figure 3), but does not noticeably alter the position of the λ_{em} value of the probe (fluctuation $\leq$3 nm; Figure 3, inset). The above results indicate that the position of the λ_{em} value of DBHA is sensitive only to polarity and not to pH and temperature, and suggest that the polarity change can be accurately detected without interference from acidity and temperature.

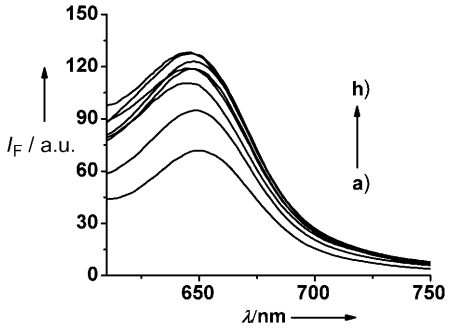

Figure 2. Effects of acidity on the fluorescence emission spectra (λ_{ex} = 585 nm) of DBHA (1 μM) at pH: a) 2.0, b) 3.0, c) 4.0, d) 5.0, e) 7.0, f) 9.0, g) 6.0, and h) 8.0.

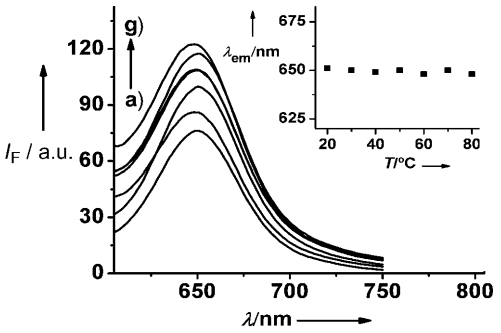

Figure 3. Effect of temperature on the fluorescence emission spectra (λ_{ex} = 585 nm) of DBHA (1 μM). The curves represent: a) 70, b) 80, c) 20, d) 30, e) 40, f) 50, and g) 60 °C. The inset shows the plot of λ_{em} versus temperature.

Modification of SOD and detection of local polarity

In this work, SOD was used as a model for studying local polarity and conformation changes. This protein is a homodimer; each subunit of SOD contains an antiparallel eight-stranded β barrel, three external loops, and a unique Tyr108 residue near the contact region.[42–46] As reported previously,[34] π-allylpalladium complexes can selectively react with a nucleophilic phenolic group under mild conditions (room temperature and near neutral media). The π-allylpalladium complex formed from the reaction between DBHA and Pd(OAc)$_2$/TPPTS would thus be expected to modify this tyrosine residue specifically (Scheme 2). Such labelling of tyrosine alone, as a model compound was also attempted (Figure S1 in the Supporting Information). The successful modification of Tyr108 can be characterized with various means, including absorption and fluorescence spectra, as well as by MALDI-TOF mass spectra.

Figure 4 shows a comparison of absorption spectra in sodium phosphate buffer. Because SOD has only one tyrosine residue and no tryptophan residues, the protein exhibits an absorption maximum only at 258 nm (curve a). The fine structure from 250 to 270 nm is attributed to phenylalanine residues.[42] On the other hand, DBHA itself gives a visible absorption maximum at 530 nm (curve b). Successful labelling could thus be characterized by the coexistence of the absorption bands from both SOD and DBHA. As can be seen, the DBHA-modified SOD exhibits a main absorption band at about 260 nm and a less intense peak at 555 nm (curve c), which correspond to the characteristic absorptions of SOD and DBHA, respectively. The new broad absorption band at about 350 nm might arise from the labelling product formed, whereas the 25 nm red shift of DBHA, once it is attached to the protein, might be the result of the change in its environment. In contrast, SOD in the control experiment in the absence of Pd(OAc)$_2$/TPPTS, displayed only the characteristic absorption of

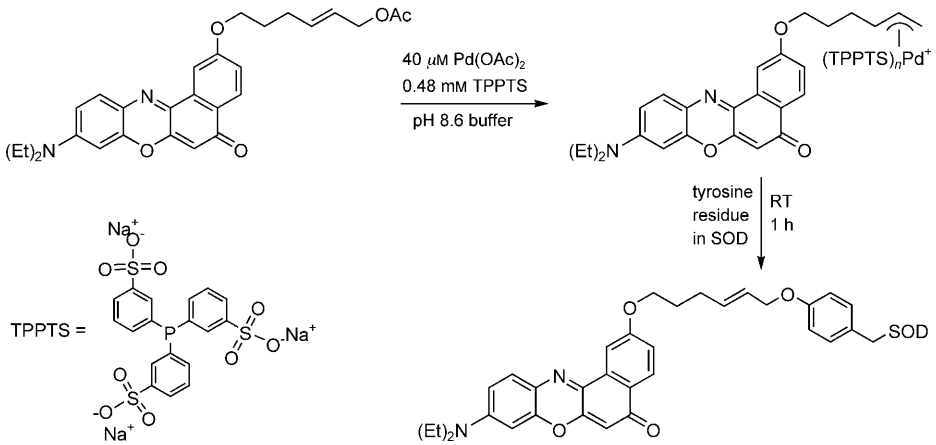

Scheme 2. Modification of Tyr108 in the bovine erythrocyte Cu/Zn superoxide dismutase (SOD) with DBHA.

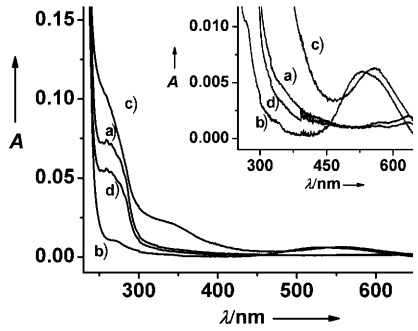

Figure 4. Comparison of absorption spectra in sodium phosphate buffer (0.1 M, pH 8.6). The curves represent: a) native SOD (7.5 μM), b) DBHA (0.1 μM), c) SOD (5 μM) modified with DBHA in the presence of $Pd(OAc)_2$/TPPTS, and d) SOD (5 μM) modified with DBHA in the absence of $Pd(OAc)_2$/TPPTS (control experiment). The inset shows a magnified section of the spectra.

SOD (curve d); this indicates that $Pd(OAc)_2$/TPPTS is indispensable for the formation of the π-allylpalladium complex intermediate for successful labelling. The labelling efficiency was 11.6%, which is calculated from the molar ratio of DBHA to SOD in the modified SOD. Namely, the concentration of DBHA can be determined from the absorbance at 530 nm ($\varepsilon_{530nm} = 5.36\times10^4\ M^{-1}cm^{-1}$), whereas the concentration of SOD is determined from the absorbance at 258 nm ($\varepsilon_{258nm} = 1.03\times10^4\ M^{-1}cm^{-1}$), from which the contribution of DBHA at 258 nm ($\varepsilon_{258nm} = 9.39\times10^4\ M^{-1}cm^{-1}$) is subtracted.

The fluorescence emission spectra of DBHA, of native SOD and of SOD modified with DBHA in the absence and presence of $Pd(OAc)_2$/TPPTS are shown in Figure 5. As noted (Table 1), DBHA exhibits an extremely weak fluorescence at 650 nm in sodium phosphate buffer (Figure 5, curve a). However, a great increase in fluorescence intensity, which was accompanied by a large blue shift of λ_{em} from 650 to 608 nm, was produced when the probe was attached to SOD (curve b). No such behaviour was observed in the control experiment (curve c). These results also support the supposition that the Tyr108 residue of SOD was successfully modified. The large blue shift ($\Delta\lambda_{em} = 42$ nm) reveals that the polarity of the Tyr108 domain

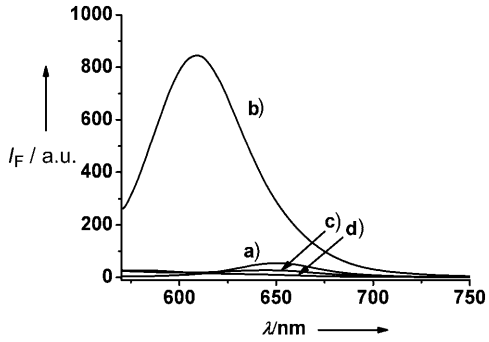

Figure 5. Comparison of fluorescence emission spectra ($\lambda_{ex} = 530$ nm) in sodium phosphate buffer. The curves represent: a) DBHA (1 μM), b) SOD (2.5 μM) modified with DBHA in the presence of $Pd(OAc)_2$/TPPTS, c) SOD (2.5 μM) modified with DBHA in the absence of $Pd(OAc)_2$/TPPTS (control experiment), and d) native SOD (5 μM).

is rather low, which would correspond to a dielectric constant of 32.6, according to the equation $\Delta\lambda_{em} = 69.4 - 0.84\times D$. The hydrophobic environment around Tyr108 might be the result of the presence of a number of nearby hydrophobic residues, such as Leu101, Ile102, Leu104, Ile110 and Ile111 (Figure S2 in the Supporting Information).[46–48] This is the first information obtained on the polarity around the Tyr108 domain.

To further confirm labelling of the protein by DBHA, the modified SOD was also subjected to MALDI-TOF mass spectrometric analysis. A peak at *m/z* 16020 (Figure S3 in the Supporting Information), which is in agreement with the theoretical value of *m/z* 16016 expected for SOD modified at its single Tyr108 residue, was detected with a mass error $< 0.02\%$; this confirms that SOD was indeed modified by DBHA. The apparent weak intensity at *m/z* 16020 can be ascribed to the low labelling efficiency.

In addition, the activity of DBHA-labelled SOD was assayed in order to examine the influence of the modification on enzyme function. The results show that the labelled SOD retains 95% of its original activity. The almost complete retention of activity might be due to the relatively long distance (14.7 Å, Figure S2 in the Supporting Information) between the labelled site and the active site; this is consistent with previous observations.[46] This also indicates that this modification method with π-allylpalladium complexes should be highly compatible with a native protein study.

Circular dichroism spectra of native SOD and DBHA-labelled SOD were recorded and compared for further study of the effects of the modification (Figure S4 in the Supporting Information). Native SOD showed a negative peak at around 212 nm; this suggests that its predominant conformation is the β sheet. The labelled SOD exhibited an almost identical CD spectrum; this indicates that the introduction of DBHA scarcely altered the secondary structure of SOD.

Acid- and heat-induced denaturation of DBHA-labelled SOD

Figure 6 shows the effect of acidity on the fluorescence spectra of DBHA-labelled SOD. As can be seen, the λ_{em} value of the DBHA-labelled SOD is almost independent of the acidity change from pH 4 to 9; this indicates that the environment

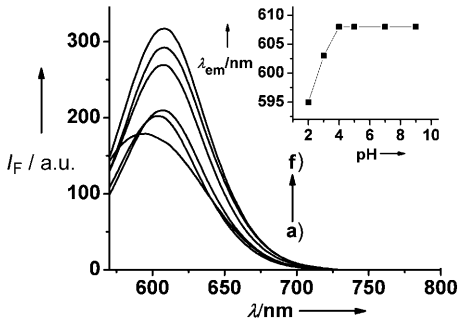

Figure 6. Fluorescence emission spectra of DBHA-labelled SOD (1 μM) in solution at various pH values. The curves represent pH: a) 2, b) 3, c) 4, d) 5, e) 7, f) 9. The inset shows the plot of λ_{em} versus pH. All spectra were recorded at $\lambda_{ex} = 530$ nm.

around Tyr108 is not affected at all. This could explain the fact that over a wider pH range—from pH 5 to 9.5—SOD maintains a stable activity in the dismutation of superoxide.[49–51] In more acidic media (from pH 4 to 2), however, the labelled SOD displayed a 13 nm blue shift in λ_{em} from 608 to 595 nm. The corresponding dielectric constant decreased from 32.6 to 17.1. This decrease in polarity indicates that strong acids can change the native folded structure of SOD and make the Tyr108 domain more hydrophobic.

Figure 7 depicts the fluorescence emission spectra and synchronous scattering spectra of DBHA-labelled SOD after different heat treatments. As shown in Figure 7A, once heated at 70 °C for 3 h, the DBHA-labelled SOD displayed a significant blue shift in λ_{em} from 608 to 579 nm, concomitant with the increase in fluorescence intensity. This indicates that the Tyr108 domain becomes rather hydrophobic, which can be ascribed to heat treatment breaking the native structure of SOD and the Tyr108 residue moving into a more hydrophobic environment.

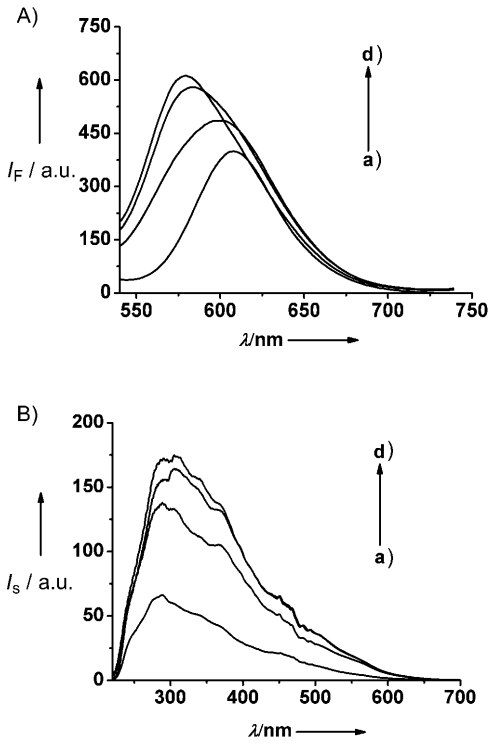

Figure 7. A) Fluorescence emission spectra (λ_{ex} = 530 nm) and B) synchronous scattering spectra of DBHA-labelled SOD (1 μM) at various heat treatments. The curves represent: a) DBHA-labelled SOD without heat treatment; and DBHA-labelled SOD with thermal denaturation at 70 °C for: b) 1 h, c) 2 h, and d) 3 h. I_s denotes the light scattering intensity.

On the other hand, the aggregation of superoxide dismutases through the formation of intermolecular disulfide bonds, as well as noncovalent interactions between β sheets, is usually observed during heat-induced denaturation.[52–54] SOD has a free thiol group at Cys6 (Figure S2 in the Supporting Information), so the protein can aggregate by disulfide bond formation,[48] which might cause Tyr108 to become buried in the highly hydrophobic region of the aggregates.[55] To confirm this speculation, aggregation of the labelled SOD during heat treatment was examined by 90° light scattering.[53,54,56,58] As shown in Figure 7B, the light scattering intensity increased gradually with increasing heating time; this indicates that aggregation of the protein does indeed occur.

DBHA binding study

A simple mixture of DBHA and SOD was examined by fluorescence spectroscopy to obtain additional information on the binding of SOD to DBHA. The experimental results show that DBHA in this simple mixture experiences a pronounced blue shift in λ_{em}, from 650 to 615 nm, concomitant with an increase in fluorescence intensity (compare curve a with curve b in Figure S5 in the Supporting Information). This indicates that the probe is bound to a hydrophobic site (with a dielectric constant of 40.9), although the position of this site in SOD is difficult to determine. However, the SOD in this simple mixture can be easily separated out with a gel filtration column (Figure S6 in the Supporting Information); this suggests that the binding of SOD to DBHA in this mixture is essentially a weak noncovalent interaction.

For comparison, the binding experiment was also performed in a different way: native SOD was first preheated at 70 °C for 60 min, and then DBHA was added. In this case, a larger blue shift of 56 nm was observed (from 650 to 594 nm; curve c in Figure S5 in the Supporting Information), in comparison with the 35 nm blue shift observed with the above simple mixture of the native SOD and DBHA. This indicates that the surface of the preheated SOD, to which DBHA binds, is more hydrophobic than that of native SOD, which is possibly the result of the formation of a more hydrophobic aggregate of SOD. Meanwhile, the formation of the aggregate was confirmed by synchronous scattering spectral analysis (Figure S7 in the Supporting Information).

Conclusions

We have developed a polarity-sensitive fluorescent probe, DBHA, for selective labelling of tyrosine residues, and the probe was employed to analyse the polarity and conformation changes of the Tyr108 domain in SOD. Acid-induced denaturation did not affect the polarity of the Tyr108 domain between pH 4 and 9, whereas heat-induced denaturation between 20 and 80 °C caused the Tyr108 domain to become more hydrophobic, which could arise from irreversible aggregation of the protein. Furthermore, probe-binding experiments revealed that thermal denaturation leads to an increase in the hydrophobicity of the protein. More applications of this approach might be expected for the detection of polarity and conformation changes of tyrosine domains in other proteins under acid- or heat-denaturation conditions.

Experimental Section

Reagents: Bovine Cu/Zn superoxide dismutase (SOD) and 4-bromobutan-1-ol (Fluka), 4-dimethylaminopyridine (Acros), superoxide dismutase detection kit (Nanjing Jiancheng Bioengineering Institute, China), diisobutylaluminium hydride (1 M solution in hexane) and (methoxycarbonylmethyl)triphenylphosphonium bromide (Alfa Aesar, Ward Hill, USA), 9-(diethylamino)-2-hydroxy-5*H*-benzo[α]phenoxazin-5-one and tris(3-sulfonatophenyl)phosphine hydrate sodium salt (TPPTS; J & K Chemical, Beijing, China), and oxalyl chloride, acetic anhydride and palladium acetate (Sinopharm Chemical Reagent, Beijing, China) were used as received. DBHA solution (5 mM) was prepared in dimethyl sulfoxide (DMSO). Unless otherwise noted, NaH_2PO_4/Na_2HPO_4 buffer (0.1 M; pH 8.6) was used in all experiments and is referred to as sodium phosphate buffer. All other chemicals used were of at least analytical grade. Deionized-distilled water was used throughout.

Apparatus: Fluorescence spectra were recorded by using a Hitachi F-2500 fluorescence spectrophotometer in (10×10) mm quartz cells (Hitachi Ltd., Tokyo, Japan) with excitation and emission slit widths of 20 nm. A model HI-98128 pH meter (Hanna Instruments Inc., Woonsocket, USA) was used for pH measurements. Absorption spectra were recorded in 1 cm cells with a Techcomp UV-8500 spectrophotometer (Shanghai, China). ^{1}H NMR and ^{13}C NMR spectra were measured with a Bruker DMX 400 spectrometer in $CDCl_3$ with tetramethylsilane as an internal standard. IR spectra were measured in KBr disks with a Bruker TENSOR 27 Fourier transform infrared spectrometer. Electrospray ionization mass spectra (ESI-MS) were measured with an LC-MS 2010A instrument (Shimadzu, Kyoto, Japan). Electron impact mass spectra (EI-MS) were obtained with a GCT mass spectrometer (Micromass, Manchester, UK). MALDI-TOF mass spectra were recorded with a BIFLEX III (Bruker, Inc.) instrument. Elemental analyses were carried out with a Flash EA1112 instrument. Circular dichroism spectra were recorded by using a Jasco J-810 spectropolarimeter at 20 °C.

Synthesis of DBHA: As depicted in Scheme 1, the probe DBHA can be synthesized by treatment of **4** with 9-(diethylamino)-2-hydroxy-5*H*-benzo[α]phenoxazin-5-one; compound **4** was prepared from 4-bromobutan-1-ol by a procedure similar to that described in the literature.[34]

Methyl 6-bromohex-2-enoate (2): A solution of anhydrous DMSO (1.4 mL, 20 mmol, 2.5 equiv) in CH_2Cl_2 (15 mL) was precooled to −78 °C and was then added dropwise at −78 °C to a solution of oxalyl chloride (1.4 mL, 16 mmol, 2 equiv) in CH_2Cl_2 (15 mL). A solution of 4-bromobutan-1-ol (8 mmol, 1 equiv) in CH_2Cl_2 (10 mL) was then slowly added to the mixture, which was stirred for 1 h at −78 °C. Freshly distilled NEt_3 (7.25 mL, 52 mmol, 6.5 equiv) was then added, and the mixture was allowed to warm to room temperature. The phosphorane (4.4 g, 13 mmol, 1.65 equiv), which was synthesized according to the literature,[34] was added to the reaction mixture. After being stirred, overnight, the orange reaction mixture was washed successively with HCl (0.1 M), saturated $NaHCO_3$, water and brine. The clear organic layer was dried with anhydrous Na_2SO_4, filtered and concentrated. The residue was purified by silica gel column chromatography (petroleum ether (b.p. 60–90 °C)/ethyl acetate, 40:1, *v/v*) to afford **2** as a pale yellow oil (1.1 g, 65% yield). ^{1}H NMR (400 MHz, $CDCl_3$): δ = 1.92–2.05 (m, 2H), 2.36–2.41 (m, 2H), 3.41 (t, J = 6.5 Hz, 2H), 3.73 (s, 3H), 5.88 (d, J = 15.7 Hz, 1H), 6.88–6.96 ppm (m, 1H); ESI-MS: *m/z* (%): 207.0 (100) $[M+H]^+$, 209.0 (97) $[M+2+H]^+$.

6-Bromohex-2-en-1-ol (3): A solution of diisobutylaluminium hydride in hexane (1.0 M, 12 mL, 12 mmol, 3 equiv) was added dropwise at −78 °C to a stirred solution of **2** (0.8 g, 4 mmol, 1 equiv) in CH_2Cl_2 (10 mL). After being stirred for 1 h at −78 °C, the solution was allowed to warm to room temperature and then saturated NH_4Cl (10 mL) was added dropwise. After the bubbling ceased, the liquid turned immediately into a clear gel. CH_2Cl_2 (10 mL) was then added to form white clumps that were removed by filtration. The organic layer was washed with brine and dried with anhydrous Na_2SO_4, overnight. After removal of the solvent by rotary evaporation, **3** was obtained as a yellow oil (0.5 g, 72% yield). ^{1}H NMR (400 MHz, $CDCl_3$): δ = 1.50 (s, 1H), 1.75–1.98 (m, 2H), 2.19–2.24 (m, 2H), 3.42 (t, J = 6.5 Hz, 2H), 4.10 (d, J = 4.4 Hz, 2H), 5.62–5.74 ppm (m, 2H); EI-MS: *m/z* (%): 178 (< 0.1) $[M]^+$, 81 (65), 71 (11), 57 (100), 43 (16), 41 (27), 39 (15), 29 (18), 27 (17).

6-Bromohex-2-enyl acetate (4): Acetic anhydride (0.5 mL, 5 mmol, 2 equiv) and 4-dimethylaminopyridine (0.02 g, 0.2 mmol, 0.08 equiv) were added successively at 0 °C to a stirred solution of **3** (0.4 g, 2.5 mmol, 1 equiv) in a pyridine/CH_2Cl_2 (1:1, *v/v*) solvent mixture. The mixture was stirred for 1 h at 0 °C and was then stirred, overnight, at room temperature. The reaction mixture was then poured into HCl (4 M, 20 mL) and extracted three times with ether (3×10 mL). The combined organic phase was washed once with dilute aqueous HCl, saturated $NaHCO_3$, water and brine. The organic layer was dried over anhydrous Na_2SO_4 and the solvent was evaporated under reduced pressure, to afford **4** as a pale yellow oil (0.4 g, 74% yield) that needed no further purification. ^{1}H NMR (400 MHz, $CDCl_3$): δ = 1.94–1.99 (m, 2H), 2.07 (s, 3H), 2.21–2.30 (m, 2H), 3.41 (t, J = 6.4 Hz, 2H), 4.52 (d, J = 5.6 Hz, 2H), 5.60–5.67 (m, 1H), 5.70–5.77 ppm (m, 1H). EI-MS: *m/z* (%): 222 (< 0.1) $[M]^+$, 180 (9.8), 178 (10), 162 (5), 160 (4.9), 141(8), 81 (39), 43 (100).

6-[9-(Diethylamino)-5-oxo-5*H*-benzo[α]phenoxazin-2-yloxy]hex-2-enyl acetate (DBHA): A mixture of **4** (0.06 g, 0.3 mmol, 1 equiv), 9-(diethylamino)-2-hydroxy-5*H*-benzo[α]phenoxazin-5-one (0.1 g, 0.3 mmol, 1 equiv) and potassium carbonate (0.1 g, 0.9 mmol, 3 equiv) in *N,N*-dimethylformamide (DMF, 3 mL) was heated at 80 °C for 2 h. The reaction mixture was then poured into water (20 mL) and extracted three times with ethyl acetate. The organic layer was dried over anhydrous Na_2SO_4 and the solvent was evaporated under reduced pressure. The resulting flaky and purple solid was purified by silica gel column chromatography (petroleum ether (b.p. 60–90 °C)/ethyl acetate, 10:1, *v/v*) to afford the product DBHA as a deep-red solid (78 mg, 57% yield). In addition, a dark-red column crystal of DBHA (Figure S8 in the Supporting Information) could be grown from the DMSO solution. ^{1}H NMR (400 MHz, $CDCl_3$): δ = 1.28 (t, J = 7.0 Hz, 6H), 1.96–2.01 (m, 2H), 2.06 (s, 3H), 2.30–2.36 (m, 2H), 3.49 (q, J = 7.0 Hz, 4H), 4.20 (t, J = 6.3 Hz, 2H), 4.55 (d, J = 6.3 Hz, 2H), 5.64–5.68 (m, 1H), 5.84–5.88 (m, 1H), 6.36 (s, 1H), 6.51 (s, 1H), 6.70 (d, J = 8.7 Hz, 1H), 7.16–7.19 (m, 1H), 7.63 (d, J = 9.0 Hz, 1H), 8.06 (s, 1H), 8.23 ppm (d, J = 8.7 Hz, 1H); ^{13}C NMR (100 MHz, $CDCl_3$): δ = 12.5, 21.0, 28.4, 28.6, 45.0, 65.0, 67.3, 96.1, 105.1, 106.4, 109.4, 118.1, 124.6, 124.7, 125.5, 127.6, 130.9, 133.9, 135.0, 139.7, 146.7, 150.6, 151.8, 161.5, 170.8, 183.1 ppm; IR: $\tilde{\nu}$ = 2973, 2933, 1737, 1600, 1500, 1409, 1314, 1229 cm^{-1}; ESI-MS: *m/z* (%): 475.3 (100) $[M+H]^+$; elemental analysis calcd (%) for $C_{28}H_{30}N_2O_5$: C 70.87, H 6.37, N 5.90%; found: C 70.82, H 6.41, N 6.11.

Crystal data for DBHA: Triclinic, space group $P\bar{1}$; a = 8.8879(18), b = 10.504(2), c = 14.014(3) Å; α = 90.67(3), β = 98.16(3), γ = 111.28(3)°; V = 1203.9(4) Å^3, Z = 2; D_{calcd} = 1.309 g cm^{-3}; T = 173(2) K; μ = 0.090 mm^{-1}; θ range = 1.47–25.00°; 7696 reflections measured, 4240 unique (R_{int} = 0.0324); GOF = 1.112, $R1$ [$I > \sigma(I)$] = 0.0679, $wR2$ (all data) = 0.1655.

Modification of Tyr108 in SOD by DBHA: The tyrosine residue was specifically modified with DBHA in the following way (Scheme 2): a solution of SOD (5 μM, 2 mL, 1 equiv) in sodium phosphate buffer (0.1 M, pH 8.6) was mixed with DBHA (5 mM, 10 μL, 5 equiv) and the catalyst/ligand solution (10 μL, prepared as described in the literature;[34] 8 equiv of $Pd(OAc)_2$, final concentration = 40 μM; and 96 equiv of TPPTS, final concentration = 0.48 mM). The mixture was stirred for 1 h at 25 °C, and was then separated on a Sephadex G-25 (Pharmacia, Uppsala, Sweden) column with sodium phosphate buffer as eluent. The protein fraction, as judged by monitoring absorbance at 258 nm with a UV-8500 spectrophotometer, was collected and stored at 4 °C. For MALDI-TOF mass spectral analysis, the collected solution was further dialysed, overnight, against NH_4HCO_3 solution (30 mM), and then lyophilized. As a control, the same procedure was performed for SOD only in the absence of the catalyst/ligand solution.

Activity measurements: The activities of both native and modified SOD were assayed by the xanthine oxidase/hydroxylamine method.[58,59] In this approach, hydroxylamine is oxidized into nitrite by the superoxide anion (O_2^-) from the reaction system, and the formed nitrite reacts with Griess' reagent to yield a mauve solution, the absorbance of which is then measured at 550 nm. Added SOD scavenges O_2^- and inhibits the oxidation, and thereby leads to a decrease in absorbance. The amount of SOD that causes 50% inhibition, under the conditions specified, is defined as one activity unit.

To determine the activity change of SOD, a mixture of xanthine oxidase, xanthine, hydroxylamine and an appropriate amount of SOD was incubated at 37 °C for 40 min. Griess' reagent was then added and the mixture was incubated for 10 min. The absorbance of the solution was measured at 550 nm in 1 cm cells against water as blank. As a control, the same procedure was performed for the reaction system only in the absence of SOD. The calculation of SOD activity (U mg^{-1}) is described by Equation (1):[58,59]

$$\text{activity of SOD} = \frac{\dfrac{A_{\text{control}} - A_{\text{unknown}}}{A_{\text{control}}} \times \dfrac{V_{\text{total}}}{V_{\text{sample}}}}{m_{\text{SOD}} \times 50\%} \quad (1)$$

where A_{control} and A_{unknown} are the absorbances of the control and the experimental sample, respectively; V_{total} and V_{sample} are the final volumes of the reaction mixture and the added SOD sample, respectively; and m_{SOD} is the amount of the added SOD (in mg).

Effect of temperature on the properties of DBHA and SOD: A solution of DBHA (1 μM) was heated at given temperatures from 20 to 80 °C and the changes in fluorescence properties were monitored. Thermal denaturation was performed by incubating the solutions of DBHA-labelled SOD (1 μM) in sodium phosphate buffer (0.1 M, pH 8.6) at 70 °C for 1, 2 and 3 h. The aggregation of SOD was monitored by 90° light scattering, and a synchronous model ($\Delta\lambda = 0$ nm) was employed with excitation and emission slit widths of 5 nm. All of the above heated samples were cooled again to room temperature for fluorescence measurements.

Effect of acidity on the properties of DBHA and SOD: A solution containing DBHA (1 μM) and NaCl (0.1 M) at different pH values (adjusted with HCl and NaOH) was used to examined the effect of acidity. The solution was incubated for 1 h at room temperature and then analysed fluorimetrically. Acid-induced denaturation was carried out by the same procedure as above, but DBHA (1 μM) was substituted with labelled SOD (1 μM) in the system.

Binding of DBHA to SOD: In binding experiments, DBHA (10 μL, 10 μM) was added to SOD (1 mL, 5 μM) in sodium phosphate buffer. The mixture was incubated at room temperature for 30 min. Then the mixture was also heated at 70 °C for either 30 or 60 min, in order to examine its denaturation behaviour. Fluorescence spectra were recorded at the corresponding optimal excitation and emission wavelengths.

Acknowledgements

We express our thanks for the financial support from the NSF of China (grant nos. 20525517, 90813032, 20875092), the 863 Program (2008AA02Z206), and the Chinese Academy of Sciences.

Keywords: analytical methods · fluorescent probes · local polarity detection · transition metals · tyrosine

[1] E. I. Solomon, J. Zhou, F. Neese, E. G. Pavel, *Chem. Biol.* **1997**, *4*, 795–808.
[2] R. Raman, V. Sasisekharan, R. Sasisekharan, *Chem. Biol.* **2005**, *12*, 267–277.
[3] F. Chiti, C. M. Dobson, *Annu. Rev. Biochem.* **2006**, *75*, 333–366.
[4] C. W. Lennon, H. D. Cox, S. P. Hennelly, S. J. Chelmo, M. A. McGuirl, *Biochemistry* **2007**, *46*, 4850–4860.
[5] E. H. Fischer, *Adv. Enzyme Regul.* **1999**, *39*, 359–369.
[6] H. P. Monteiro, *Free Radical Biol. Med.* **2002**, *33*, 765–773.
[7] C. Grangeasse, A. J. Cozzone, J. Deutscher, I. Mijakovic, *Trends Biochem. Sci.* **2007**, *32*, 86–94.
[8] I. Tietzel, D. M. Mosser, *Front. Biosci.* **2002**, *7*, d1494–1502.
[9] J. H. Cho, D. H. Kim, D. Kim, K. J. Lee, K. Y. Choi, *Biochemistry* **2001**, *40*, 10197–10203.
[10] A. Teplyakov, K. S. Wilson, P. Orioli, S. Mangani, *Acta Crystallogr. Sect. D* **1993**, *49*, 534–540.
[11] E. Deprez, E. Gill, V. Helms, R. C. Wade, G. Hui Bon Hoa, *J. Inorg. Biochem.* **2002**, *91*, 597–606.
[12] A. Okamoto, K. Tanaka, T. Fukuta, I. Saito, *ChemBioChem* **2004**, *5*, 958–963.
[13] E. Sharon, S. A. Lvesque, M. N. Munkonda, J. Svigny, D. Ecke, G. Reiser, B. Fischer, *ChemBioChem* **2006**, *7*, 1361–1374.
[14] O. Wichmann, M. H. Gelb, C. Schultz, *ChemBioChem* **2007**, *8*, 1555–1569.
[15] F. Krieger, A. Mourot, R. Araoz, F. Kotzyba-Hibert, J. Molg, E. Bamberg, M. Goeldner, *ChemBioChem* **2008**, *9*, 1146–1153.
[16] P. Marek, R. Gupta, D. P. Raleigh, *ChemBioChem* **2008**, *9*, 1372–1374.
[17] C. Losasso, E. Cretaio, K. Palle, L. Pattarello, M. Bjornsti, P. Benedetti, *J. Biol. Chem.* **2007**, *282*, 9855–9864.
[18] B. E. Cohen, T. B. McAnaney, E. S. Park, Y. N. Jan, S. G. Boxer, L. Y. Jan, *Science* **2002**, *296*, 1700–1703.
[19] X. J. Duan, Z. W. Zhao, J. P. Ye, H. M. Ma, A. D. Xia, G. Q. Yang, C. Wang, *Angew. Chem.* **2004**, *116*, 4312–4315; *Angew. Chem. Int. Ed.* **2004**, *43*, 4216–4219.
[20] S. Y. Dong, H. M. Ma, X. J. Duan, X. Q. Chen, J. Li, *J. Proteome Res.* **2005**, *4*, 161–166.
[21] S. Y. Dong, Z. W. Zhao, H. M. Ma, *J. Proteome Res.* **2006**, *5*, 26–31.
[22] Z. J. Bao, S. J. Wang, W. Shi, S. Y. Dong, H. M. Ma, *J. Proteome Res.* **2007**, *6*, 3835–3841.
[23] J. Nakanishi, T. Nakajima, M. Sato, T. Ozawa, K. Tohda, Y. Umezawa, *Anal. Chem.* **2001**, *73*, 2920–2928.
[24] S. Ercelen, A. S. Klymchenko, A. P. Demchenko, *FEBS Lett.* **2003**, *538*, 25–28.
[25] R. B. Spruijt, A. B. Meijer, C. Wolfs, M. A. Hemminga, *Biochim. Biophys. Acta Biomembr.* **2000**, *1509*, 311–323.
[26] B. E. Cohen, A. Pralle, X. J. Yao, G. Swaminath, C. S. Gandhi, Y. N. Jan, B. K. Kobilka, E. Y. Isacoff, L. Y. Jan, *Proc. Natl. Acad. Sci. USA* **2005**, *102*, 965–970.

[27] R. L. Lundblad, *Chemical Reagents for Protein Modification*, 3rd ed., CRC, Boca Raton, **2005**, Chapter 9.
[28] J. F. Riordan, B. L. Vallee, *Methods Enzymol.* **1972**, *25*, 494–499.
[29] D. Karibian, C. Jones, A. Gertler, K. J. Dorrington, T. Hofmann, *Biochemistry* **1974**, *13*, 2891–2897.
[30] M. Sokolovsky, J. F. Riordan, B. L. Vallee, *Biochemistry* **1969**, *8*, 4740–4745.
[31] M. Tabachnick, H. Sobotka, *J. Biol. Chem.* **1960**, *235*, 1051–1054.
[32] T. J. Tsomides, H. N. Eisen, *Anal. Biochem.* **1993**, *210*, 129–135.
[33] J. M. Antos, M. B. Francis, *Curr. Opin. Chem. Biol.* **2006**, *10*, 253–262, and references therein.
[34] S. D. Tilley, M. B. Francis, *J. Am. Chem. Soc.* **2006**, *128*, 1080–1081.
[35] C. M. Golini, B. W. Williams, J. B. Foresman, *J. Fluoresc.* **1998**, *8*, 395–404, and references therein.
[36] K. Nagy, S. Göktük, L. Biczók, *J. Phys. Chem. A* **2003**, *107*, 8784–8790.
[37] J. R. Lakowicz, *Principles of Fluorescence Spectroscopy*, 2nd ed., Kluwer Academic/Plenum, New York, **1999**, Chapter 6.
[38] A. Okamoto, K. Tainaka, Y. Fujiwara, *J. Org. Chem.* **2006**, *71*, 3592–3598.
[39] J. A. Dean, *Lange's Chemistry Handbook*, 15th ed., McGraw-Hill, New York, **1999**, pp. 5.105–5.129.
[40] J. N. Demas, G. A. Crosby, *J. Phys. Chem.* **1971**, *75*, 991–1024.
[41] T. Karstens, K. Kobs, *J. Phys. Chem.* **1980**, *84*, 1871–1872.
[42] J. M. McCord, I. Fridovich, *J. Biol. Chem.* **1969**, *244*, 6049–6055.
[43] J. L. Abernethy, H. M. Steinman, R. L. Hill, *J. Biol. Chem.* **1974**, *249*, 7339–7347.
[44] J. A. Tainer, E. D. Getzoff, K. M. Beem, J. S. Richardson, D. C. Richardson, *J. Mol. Biol.* **1982**, *160*, 181–217.
[45] H. Oneda, K. Inouye, *J. Biochem.* **2003**, *134*, 683–690.
[46] M. A. Hough, S. S. Hasnain, *J. Mol. Biol.* **1999**, *287*, 579–592.
[47] L. Banci, I. Bertini, F. Cramaro, R. D. Conte, M. S. Viezzoli, *Eur. J. Biochem.* **2002**, *269*, 1905–1915.
[48] D. E. McRee, S. M. Redford, E. D. Getzoff, J. R. Lepock, R. A. Hallewell, J. A. Tainer, *J. Biol. Chem.* **1990**, *265*, 14234–14241.
[49] G. Rotilio, L. Morpurgo, C. Giovagnoli, L. Calabrese, B. Mondovi, *Biochemistry* **1972**, *11*, 2187–2192.
[50] J. V. Bannister, W. H. Bannister, G. Rotilio, *CRC Crit. Rev. Biochem.* **1987**, *22*, 111–180.
[51] L. M. Ellerby, D. E. Cabelli, J. A. Graden, J. S. Valentine, *J. Am. Chem. Soc.* **1996**, *118*, 6556–6561.
[52] S. D. Khare, M. Caplow, N. V. Dokholyan, *Proc. Natl. Acad. Sci. USA* **2004**, *101*, 15094–15099.
[53] P. B. Stathopulos, J. A. O. Rumfeldt, G. A. Scholz, R. A. Irani, H. E. Frey, R. A. Hallewell, J. R. Lepock, E. M. Meiering, *Proc. Natl. Acad. Sci. USA* **2003**, *100*, 7021–7026.
[54] L. Banci, I. Bertini, A. Durazo, S. Girotto, E. B. Gralla, M. Martinelli, J. S. Valentine, M. Vieru, J. P. Whitelegge, *Proc. Natl. Acad. Sci. USA* **2007**, *104*, 11263–11267.
[55] G. Gotte, F. Vottariello, M. Libonati, *J. Biol. Chem.* **2003**, *278*, 10763–10769.
[56] B. A. Chrunyk, R. Wetzel, *Protein Eng.* **1993**, *6*, 733–738.
[57] M. D. de Beus, J. Chung, W. Colón, *Protein Sci.* **2004**, *13*, 1347–1355.
[58] J. P. Ji, Z. B. Wu, Q. S. Liu, Y. S. Zhang, M. Ye, M. J. Li, *J. Nanjing Rail. Med. Coll.* **1991**, *10*, 27–30.
[59] Y. J. Ji, C. B. Yue, Chin, Patent No. CN 92107634.7, **1992**.

Received: January 4, 2009
Published online on April 9, 2009

